

PARABOLIC BURSTING IN AN EXCITABLE SYSTEM COUPLED WITH A SLOW OSCILLATION*

G. B. ERMENTROUT[†] AND N. KOPELL[‡]

Abstract. We investigate the interaction of an excitable system with a slow oscillation. Under robust and general assumptions compatible with the more stringent assumptions usually made about excitable systems, we show that such a coupled system can display bursting, i.e. a stable solution in which some variable undergoes rapid oscillations followed by a period of quiescence, with both oscillation and quiescence continually repeated. Under a further weak condition, the bursting is “parabolic”, i.e. the local frequency of the fast oscillation increases and then decreases within a burst. The technique in this paper involves nonlinear changes of coordinates which transform the equations into ones which are closely related to Hill’s equation.

Key words. parabolic bursting, excitable system, oscillation

AMS(MOS) subject classifications. 58F22, 92A09

1. Introduction. The term “bursting” refers to the dynamic behavior in which some variable undergoes rapid oscillations followed by a period of quiescence, with both oscillation and quiescence continually repeated. This behavior is found in many electrically excitable biological systems (see [1], [2] for references) as well as in chemical reactions [3], [4], [5].

In a number of the biological systems, the bursting appears to have extra structure. There is an underlying “slow wave” which modulates the frequency and amplitude of the fast oscillating bursts. High frequency spikes or action potentials appear to “ride” the maxima of the slow oscillations, resulting in burst-like structure. The interspike intervals within a burst are not constant; the initial intervals are long, then they decrease and finally increase again. Such a pattern is called parabolic bursting. (For a picture see [6].)

The purpose of this paper is to present a mathematical mechanism for parabolic bursting that describes the interaction of a slow oscillation with an excitable system. The hypotheses are very weak and are compatible with the more stringent assumptions usually made about excitable systems. For reasons important in the applications of these results (to modelling of the aplysia abdominal ganglion and smooth muscle, to be done in a companion paper [7], and to pairs of neurons in, e.g. the lobster stomatogastric ganglion) we allow the slow oscillation to be significantly affected by the excitable system, so we are not describing merely a slowly forced excitable system. We show that, under very general conditions, one gets parabolic bursting as well as the more regular rapid oscillations known as “beating”.

The present article is organized as follows: In § 2, a general mechanism is described, and we explain why our assumptions on the excitable system can be satisfied by Hodgkin–Huxley like models of membranes. Section 3 contains the bulk of the mathematical results. It is shown that a large class of equations which embody this mechanism is transformable by successive nonlinear changes of coordinates to

* Received by the editors December 10, 1984, and in revised form April 17, 1985.

[†] Department of Mathematics, University of Pittsburgh, Pittsburgh, Pennsylvania 15260. The work of this author was supported by the National Science Foundation under grant MCS 8300885.

[‡] Department of Mathematics, Northeastern University, Boston, Massachusetts 02115. The work of this author was supported by the National Science Foundation under grant MCS 8301249 and by the J. S. Guggenheim Foundation.

equations which contain (in some nonuniform limit) Hill's equation. The stability diagram associated with Hill's equation then turns out to give information about bursting and beating. Section 4 contains an example of a Hill equation that is analyzed completely, and it is shown how transitions between different bursting patterns occur. The final section is a discussion which relates our results to other mechanisms for bursting, and to experimentally observed bursting phenomena in the Belousov-Zhabotinskii reaction [3], [4]. We also discuss applications not contained in [7].

2. A mathematical mechanism for bursting. The class of models to be analyzed is quite abstract with very few hypotheses. The equations are:

$$(2.1) \quad \dot{x} = f(x) + \varepsilon^2 g(x, y, \varepsilon),$$

$$(2.2) \quad \dot{y} = \varepsilon h(x, y, \varepsilon)$$

where $x \in \mathbb{R}^p$, $y \in \mathbb{R}^q$, $\varepsilon \ll 1$ and f, g, h are smooth (e.g. C^∞) functions. The hypotheses are as follows:

(A) $\dot{x} = f(x)$ has an attracting invariant circle with a single critical point (a sink-saddle). This critical point is at $x = 0$.

(B) $\dot{y} = h(0, y, 0)$ has a stable limit cycle solution.

The variable x in (2.1), (2.2) will be interpreted as the vector of transmembrane potential and ionic gates that are used to describe the dynamics of electrically excitable tissue. The vector y consists of the slowly oscillating variables which underly the bursting. (For the applications to be discussed in [7], the slow oscillation we have in mind is cytoplasmic, involving electrochemical processes not in the cell membrane. This sharply differentiates our mechanism from most accounts of bursting which make use only of properties of the cell membrane [8], [9].) Thus, x generates the spikes and y generates the slow waves. The function g represents the coupling of the slow waves to the spiking mechanisms.

It is obvious that (2.2) and Hypothesis B imply the existence of a slow oscillation. What is not so clear is how (2.1) and Hypothesis A describe an electrically excitable system. We now show how this situation arises in a natural way from the properties of Hodgkin-Huxley like equations. None of the phenomena to which the model is intended to apply involve spatial propagation. Thus, we start with the "space-clamped" system. One such version of the equations has the form:

$$(2.3) \quad C \frac{dV}{dt} = -G(V, m, n),$$

$$(2.4a) \quad \frac{dm}{dt} = \bar{\delta}(m_\infty(V) - m) / \tau_m(V),$$

$$(2.4b) \quad \frac{dn}{dt} = \bar{\varepsilon}(n_\infty(V) - n) / \tau_n(V).$$

Here, $V(t)$ is the transmembrane potential and m and n are vectors of "activators" or "inhibitors" of gates allowing ionic currents to flow inward or outward. For example, in the classic Hodgkin-Huxley equations, there are two variables for sodium current (outward) and one for potassium current (inward). In (2.4), the gates have been separated into those which equilibrate quickly ($\bar{\delta} \gg 1$) and those which act slowly ($\varepsilon \ll \bar{\varepsilon} \ll 1$, i.e., slow equilibration, but not as slow as the "slow" oscillation underlying the bursts). In the standard Hodgkin-Huxley equations, g is linear in V ; however the

full system is very nonlinear. (2.3) and (2.4) are generally simplified by the use of a pseudo steady state hypothesis: since \dot{m} is large, m approaches $m_\infty(V)$ quickly, so (2.3) is approximated by replacing m by $m_\infty(V)$. (The elimination of the fast variable can be justified by using invariant manifold theory, e.g., [11].) The resulting function, $\bar{G}(V, n) \equiv G(V, m_\infty(V), n)$ is assumed to have a “cubic” shape as a function of V (for fixed n) [8], [12], [13], [14], [15].

For purposes of clarity, assume first that n is one-dimensional so that the reduced system ($m = m_\infty(V)$) is two-dimensional. The most important of the slow gates is potassium activation, so we associate n with this process. The curve $n_\infty(V)$ is typically “S” shaped (like hyperbolic tangent), monotone increasing with small slope for V very large or very small and large slope when V is intermediate in value. The null clines for the reduced system are shown in Figs. 2.1a and 2.1b. Three of the possible phase

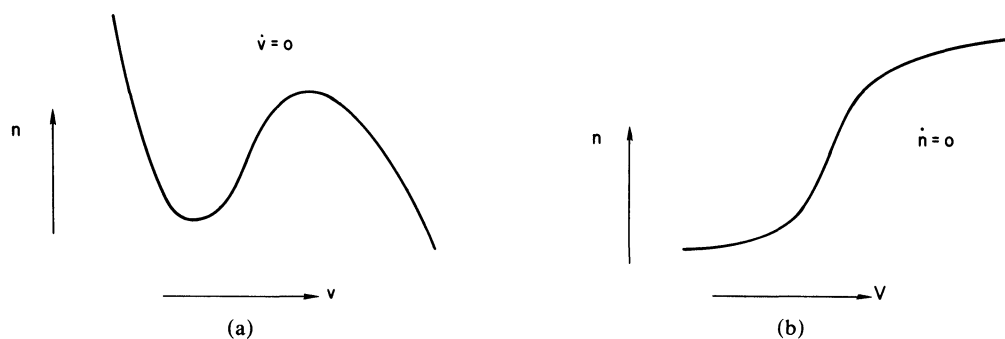


FIG. 2.1. Null clines for the reduced Hodgkin-Huxley system. (a) Voltage null-cline. (b) Recovery null-cline.

planes to the reduced system are shown in Figs. 2.2a, 2.2b and 2.2c. In Fig. 2.2a, there is a stable periodic solution which can be viewed as an invariant circle with no critical points. In Fig. 2.2b, there is in addition to the unstable source, a stable critical point and a saddle point. This type of system is often called “excitable”; a small perturbation in V above a certain threshold leads to a trajectory which makes a large excursion before returning to rest. In this case there is also a stable invariant circle which is the closure of the unstable manifold of (i.e., trajectory leaving) the saddle point. On this circle there are two critical points; one is stable corresponding to the stable rest point and the other is unstable, corresponding to the saddle point. For this type of system, the transition from oscillatory activity to excitability (Fig. 2.2a to Fig. 2.2b) involves a bifurcation on the invariant circle in which a pair of critical points are born. (The existence of a smooth invariant attracting circle for the system of Fig. 2.2b is guaranteed close to the bifurcation point by the existence and stability in the system of Fig. 2.2a. For, by invariant manifold theory [16], the smooth attracting circle cannot disappear when Fig. 2.2a is perturbed, even if critical points appear on the circle, until eigenvalues at the new critical points are comparable in size to the rate of normal attraction to the circle.) This type of transition and this model for excitability were used in [17] to study waves in an excitable or oscillatory medium. At the end of this section, we list some models which exhibit this transition. At the bifurcation point (Fig. 2.2c), the system satisfies Hypothesis A and is on the boundary between excitability and periodicity. Note that in (2.1), $g(x, y, 0)$ may contain terms independent of y ; hence $\dot{x} = f(x)$ could be replaced by an equation which is a small amount ($O(\epsilon^2)$) on either side of the boundary.

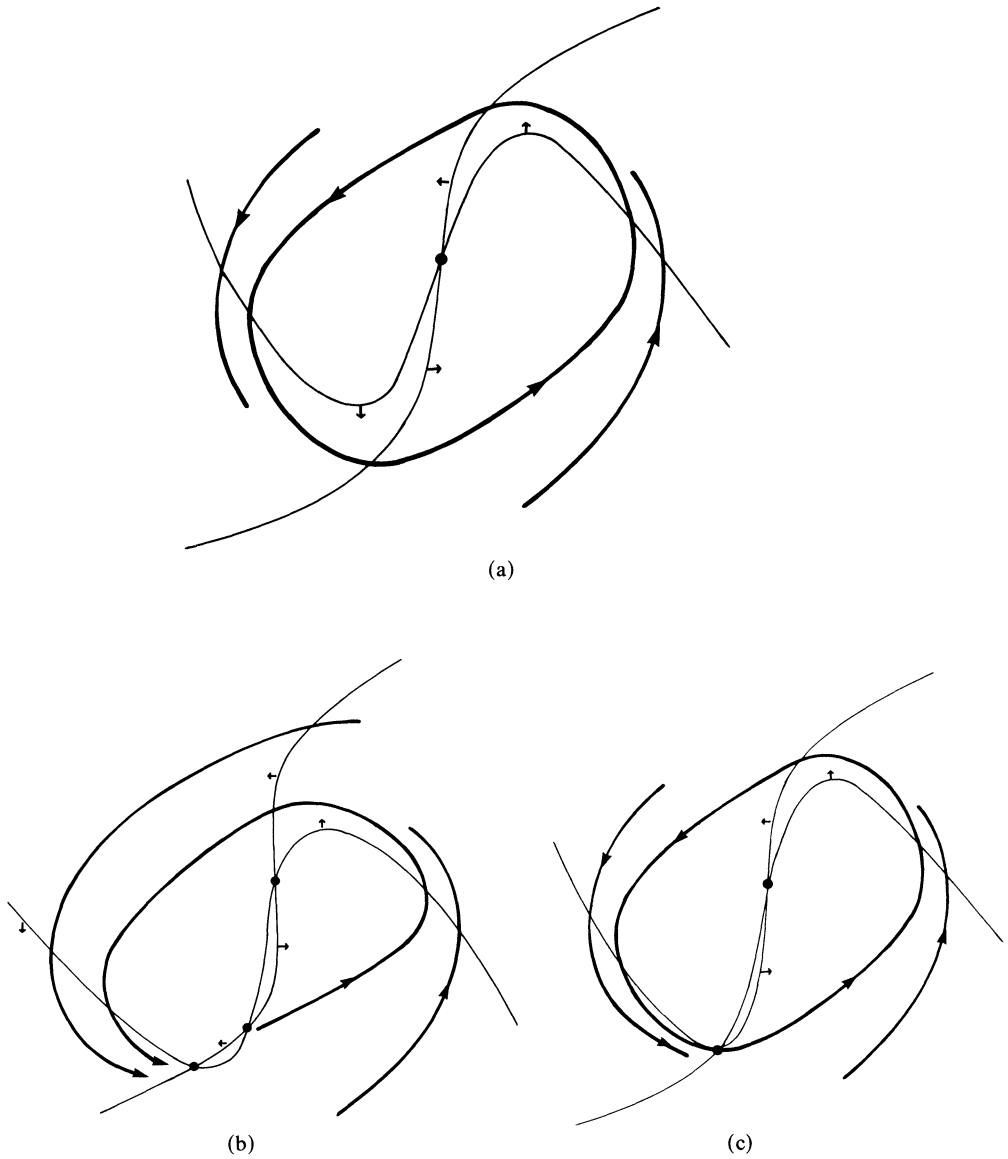


FIG. 2.2. Phase portraits of the reduced Hodgkin-Huxley system for various parameter values. (a) Stable oscillation. (b) Excitable. (c) Criticality.

The following simple example of a system on the unit circle illustrates these bifurcations:

$$(2.5) \quad \frac{d\theta}{dt} = (1 - \cos \theta) + a(1 + \cos \theta), \quad \theta \in S^1.$$

For $a > 0$, $d\theta/dt$ is > 0 and the variable θ moves continuously around the circle. For $a < 0$, there are two singular points, one stable and one unstable. (For a small they are $\pm 2\sqrt{|a|}$ respectively.) Thus, $a = 0$ is the bifurcation point; $\theta = 0$ is the unique critical point on the circle.

We remark that in (2.1), the forcing terms $\varepsilon^2 g(x, y, \varepsilon)$ appear to be much smaller than the right-hand side of (2.2). However, in some applications, $g(x, y, \varepsilon)$ can be quite sizable, for example, when there are many spikes per burst. This is discussed further after Lemma 4 of § 3.

While we have shown how the behavior desired can arise from somewhat abstract Hodgkin–Huxley type equations, we list here some systems in which it has actually been found within the parameter ranges prescribed by the investigators of these systems. Rall and Shepherd proposed a 3-variable model for impulse propagation in mitral cells, the kinetics of which show exactly this behavior [18]. Hastings [19], in discussing certain discrete models, shows that the Tuckwell–Miura model for spreading depression [20] satisfies Hypothesis A. In [21] travelling waves are found in a model of corticothalamic interactions. A study of the phase plane for the 2-variable “space-clamped” system shows that excitability occurs via the mechanism discussed above. Finally, Rinzel and Ermentrout (unpublished) found that Connor’s model for class I axons [12] (first described by Huxley [22]) has dynamics which are close to this mechanism.

3. Beating and bursting. In addition to bursting, electrically excitable cells also display behavior known as “beating”, which denotes regular rapid oscillations. The same cell under different conditions can burst or beat [23]. In this section, we show that (2.1) and (2.2) embed in a natural way in a two-parameter family of equations; for different values of the parameters, the solutions can display beating or bursting with different numbers of spikes per burst. For some range of the parameters, there are no spikes and only the slow oscillation is evident. When there are spikes, they occur only in a limited interval of phases of the slow oscillation, the interval depending on the parameter values. These assertions and others are made explicit in the following series of lemmas.

Lemma 1 says that the stability of the invariant circle, S^1 , for $\dot{x} = f(x)$ allows one to ignore all the x -variables except one, denoted x_1 , which parametrizes S^1 . This means that (2.1) and (2.2) can be reduced from an equation on $\mathbb{R}^p \times \mathbb{R}^q$ to one on $S^1 \times \mathbb{R}^q$. The lemma is quite technical, the difficulty arising from the noncompactness of y which forces one to construct only a “local” invariant manifold. (Because of the stability of the limit cycle solution to $\dot{y} = h(0, y, 0)$, this construction is all that is required.)

LEMMA 1. *Let $N_1 \subset \mathbb{R}^q$ be any precompact neighborhood of the image L of the limit cycle of $\dot{y} = h(0, y, 0)$. There is a neighborhood N of S^1 in \mathbb{R}^p and $\varepsilon_0 > 0$ such that for $\varepsilon \leq \varepsilon_0$, there is a $(q + 1)$ -dimensional submanifold $M(\varepsilon) \subset N \times N_1 \equiv U$, parametrized by x_1 and $y \in N_1$ with the property that if $(x(t), y(t))$ satisfies (2.1), (2.2) with $(x(0), y(0)) \in M(\varepsilon)$, and $(x(t), y(t)) \in U$ for $t \leq t_0$, then $(x(t), y(t)) \in M(\varepsilon)$ for $t \leq t_0$. (I.e., $M(\varepsilon)$ is a local invariant manifold.) Furthermore, $M(\varepsilon)$ is locally attracting: if $(x(t), y(t)) \in U$ for all $t \geq 0$, then the distance from $(x(t), y(t))$ to $M(\varepsilon)$ goes to zero as $t \rightarrow \infty$.*

Proof. The assertion follows from the invariant manifold theory as described in Fenichel [16]. By hypothesis, S^1 is an attracting invariant circle of (2.1) for $\varepsilon = 0$. Thus, when $\varepsilon = 0$, $S^1 \times \mathbb{R}^q$ is invariant and attracting for (2.1) and (2.2). The result we wish follows from the persistence of attracting invariant manifolds under perturbations [16]. However, to apply [16], we must restrict ourselves to a compact subset of \mathbb{R}^q (e.g. $c1(N_1)$) and modify the equations to achieve a technical condition known as “overflowing invariance”. Let $N \subset \mathbb{R}^p$ be any precompact neighborhood of S^1 such that the vector field $\dot{x} = f(x)$ points inward on ∂N . Let N_2, N_3 be open sets $\subset \mathbb{R}^q$ with $c1(N_1) \subset N_2$, $c1(N_2) \subset N_3$. Modify (2.2) on $\mathbb{R}^p \times (N_3 - N_1)$ such that, for all ε sufficiently small (including $\varepsilon = 0$), the new vector field points outward on $\{x\} \times \partial N_2$ for all $x \in N$. (In the unmodified equations, at $\varepsilon = 0$, the vector field is tangent to $\{x\} \times \partial N_2$, since $\dot{y} = 0$.)

The results of [16] then imply that for $\varepsilon > 0$ small enough, there is an attracting invariant manifold $\bar{M}(\varepsilon)$ close to $S^1 \times N_2$. Since the equations are unperturbed on $N \times N_1$, a subset $M(\varepsilon)$ is a local invariant manifold for (2.1) and (2.2). ($M(\varepsilon)$ depends on the modification on $N_3 - N_1$ and can be made arbitrarily smooth by making the modifications small enough.) \square

On $M(\varepsilon)$ (2.1) and (2.2) have the form

$$(3.1) \quad x_1 = \bar{f}(x_1) + \varepsilon^2 \bar{g}(x_1, y, \varepsilon), \quad x_1 \in S^1,$$

$$(3.2) \quad \dot{y} = \varepsilon \bar{h}(x_1, y, \varepsilon), \quad y \in \mathbb{R}^q.$$

Suppose $S^1 = [-1, +1]/(\{-1\} = \{1\})$, with $x_1 = 0$ the critical point of $\dot{x}_1 = \bar{f}(x_1)$. The next lemma gives a change of coordinates, $x_1 = A(\theta, \varepsilon)$, whose inverse takes S^1 on to another circle, $\bar{S}_1 = [-\pi, \pi]/(\{-\pi\} = \{\pi\})$, and which maps a small neighborhood of $x_1 = 0$ onto all but a small neighborhood of $\theta = \pi$ in \bar{S}_1 . In the limit (nonuniform) as $\varepsilon \rightarrow 0$, equations written in these coordinates depend only on $\bar{g}(0, y, 0)$ and $\bar{h}(0, y, 0)$.

LEMMA 2. *There exists a change of coordinates, $x_1 = A(\theta, \varepsilon)$ and a constant, c , such that in coordinates $\theta, y, \tau \equiv \varepsilon t$, (3.1) and (3.2) converge pointwise as $\varepsilon \rightarrow 0$ to the equations*

$$(3.3) \quad \frac{d\theta}{d\tau} = (1 - \cos \theta) + (1 + \cos \theta) \bar{g}(0, y, 0),$$

$$(3.4) \quad \frac{dy}{d\tau} = \frac{1}{c} \bar{h}(0, y, 0),$$

for all $\theta \neq \pi$. The convergence is uniform except near $\theta = \pi$.

Proof. First, let c be defined by $\bar{f}(x_1) - cx_1^2 = O(x_1^3)$ near $x_1 \equiv 0$. (Recall that $\bar{f}(0) = \bar{f}'(0) = 0$ by construction.) For $|x_1| \leq \sqrt{\varepsilon}$, $A(\theta, \varepsilon)$ is defined by $x_1 = \varepsilon \tan(\theta/2)$. This transformation takes $|x_1| < \sqrt{\varepsilon}$ onto the neighborhood $|\theta| \leq 2 \tan^{-1}(1/\sqrt{\varepsilon})$. Now $2 \tan^{-1}(1/\sqrt{\varepsilon}) \rightarrow \pi$ as $\varepsilon \rightarrow 0$. Indeed $2 \tan^{-1}(1/\sqrt{\varepsilon}) = \pi - 2\sqrt{\varepsilon} + O(\varepsilon)$. (This can be seen, for example, by the identity

$$\int_1^x \frac{dt}{1+t^2} = \int_{1/x}^1 \frac{dt}{1+t^2} \quad)$$

For $|x_1| > \sqrt{\varepsilon}$, $x_1 = A(\theta, \varepsilon)$ is extended to a map $\bar{S}_1 \rightarrow S^1$ such that

(i) $A(\theta, \varepsilon)$ is a smooth one-to-one map of \bar{S}_1 onto S^1 with a smooth inverse.

(ii) For fixed $\varepsilon > 0$ sufficiently small, at any point in $[-2 \tan^{-1}(1/\sqrt{\varepsilon}), 2 \tan^{-1}(1/\sqrt{\varepsilon})]$, in the new variables, we have $d\theta/d\tau \geq 1$. (This property is needed for Lemma 4.)

These two conditions can be satisfied. For at $x_1 = \sqrt{\varepsilon}$ or, equivalently, $\theta = 2 \tan^{-1}(1/\sqrt{\varepsilon})$,

$$\frac{\partial A}{\partial \theta} = \frac{\varepsilon}{2} \sec^2 \left(\tan^{-1} \left(\frac{1}{\sqrt{\varepsilon}} \right) \right) = \frac{1}{2} + O(\varepsilon)$$

and

$$\frac{dx_1}{d\tau} = 1 + O(\varepsilon).$$

Since

$$(3.5) \quad \frac{\partial A}{\partial \theta} \frac{d\theta}{d\tau} = \frac{dx_1}{d\tau},$$

at $x_1 = \sqrt{\varepsilon}$ we have $d\theta/d\tau = 2 + O(\varepsilon)$. Furthermore, for any fixed δ (independent of ε), $dx_1/d\tau|_{x_1=\delta} = O(1/\varepsilon)$ where the latter estimate is over any compact neighborhood for y . Since A has to stretch an interval of size $4\sqrt{\varepsilon} + O(\varepsilon)$ over an interval of size $2 - 2\sqrt{\varepsilon}$ (an average stretch of $1/2\sqrt{\varepsilon} + O(\varepsilon)$), it is easy to choose $A(\theta, \varepsilon)$ so that

$$\frac{\partial A}{\partial \theta} \cong \min_{y \in N_1} \left\{ \frac{dx_1}{d\tau} \Big|_{x_1=A(\theta, \varepsilon)} \right\}.$$

Recall that N_1 is a precompact set in \mathbb{R}^q containing in its interior the image L of the periodic solution to (3.4). It then follows from (3.5) that $d\theta/d\tau \cong 1$ when y remains in N_1 .

We now consider (3.1) and (3.2) in the new variables. For $|x_1| < \sqrt{\varepsilon}$, using standard trigonometric identities, we find:

$$(3.6) \quad \frac{d\theta}{d\tau} = (1 - \cos \theta) + (1 + \cos \theta)[\bar{g}(0, y, 0)] + R_1$$

where $R_1 \cong O(\sqrt{\varepsilon})$ for $|\varepsilon \tan \theta/2| \cong \sqrt{\varepsilon}$. For any $\theta \neq \pi$, $|\varepsilon \tan \theta/2| \cong \sqrt{\varepsilon}$ when ε is small enough, so (3.6) converges to (3.3) uniformly for all θ outside a neighborhood of π . Equation (3.4) is immediate from (2.2) and $|x_1| < \sqrt{\varepsilon}$. \square

The convergence of (3.1) and (3.2) to (3.3) and (3.4) does not automatically imply the convergence of the solutions of the former to those of the latter, especially since, for most of the interesting solutions, the trajectories must pass many times through $\theta = \pi$, where our full equations do not converge to the reduced ones. This issue is resolved in Lemma 4. We turn first to the solutions to (3.3) and (3.4). The next lemma shows that these equations display the qualitative behavior which, reinterpreted in terms of the original variables, corresponds to beating and parabolic bursting. This behavior and other finer structure is detected by means of another change of coordinates which turns (3.3) and (3.4) into Hill's equation. The natural embedding of (3.3) and (3.4) (and hence of (3.1) and (3.2)) into a two-parameter family comes from the two parameters in Hill's equation.

Before stating Lemma 3, we note that there is an attracting invariant submanifold for (3.3) and (3.4) which is a two-dimensional torus. That is, (3.4) decouples from (3.3) and, by hypothesis, has an attracting limit cycle we previously called L ; the torus is $\bar{S}_1 \times L \subset \bar{S}_1 \times \mathbb{R}^q$. (The equations (3.1) and (3.2) with $\varepsilon \neq 0$ do not necessarily have such an invariant torus.) If $y(\tau)$ is a periodic solution to (3.4) lying on L , then on the invariant torus, (3.3) may be written as

$$(3.7) \quad \frac{d\theta}{d\tau} = (1 - \cos \theta) + (1 + \cos \theta)[\bar{g}(0, y(\tau), 0)],$$

a time-dependent system with periodic coefficients. For such a differential equation on a torus, we can associate a rotation number [24] which gives the average number of times a solution goes around \bar{S}_1 in an interval of time T , where T is the minimum period of $y(\tau)$. (The rotation number is independent of initial conditions and can be any real number.)

LEMMA 3. Equation (3.7) embeds in a two-parameter family of equations

$$(3.8) \quad \frac{d\theta}{d\tau} = F_{\alpha, \beta}(\theta, \tau)$$

for which there is a countable number of regions in parameter space, labelled P_j and C_j , $j = 0, 1, 2, \dots$ having the following properties:

(i) For $\alpha, \beta \in P_j$, (3.8) is structurally stable, with one stable limit cycle that is globally attracting except for points on an unstable limit cycle. The limit cycles wind j times around \bar{S}_1 and once around L . (Thus, the periodic output is the j th superharmonic of the forcing term.)

(ii) On the boundary of P_j , the stable and unstable limit cycles coalesce and disappear.

(iii) For $\alpha, \beta \in C_j$, the flow on (3.2) is equivalent to parallel flow on the torus with a rotation number $\rho(\alpha, \beta)$ between j and $j + 1$.

Proof. The assertions follow from the properties of Hill's equation which we get from the transformation

$$(3.9) \quad -\frac{V_\tau}{V} = \tan(\theta/2).$$

We write

$$(3.10) \quad \bar{g}(0, y(\tau), 0) = \alpha + \beta H(\tau)$$

where α is the mean of $\bar{g}(0, y(\tau), 0)$ over one period T , H has a mean of zero, and $\max |H(\tau)| = 1$. Then (3.8) becomes:

$$(3.11) \quad V_{\tau\tau} = -[\alpha + \beta H(\tau)]V.$$

For a particular $\bar{g}(0, y(\tau), 0)$, α and β are fixed; the two-parameter family (3.8) is obtained by allowing these parameters to vary.

It is well known [24], [25] that in (3.11), the (α, β) -plane may be divided into countably many stability regimes (see Fig. 3.1). Let P_j denote the j th instability regime, for which the Floquet multipliers of (3.11) are real; C_j denotes the j th stability regime, for which the Floquet exponents are pure imaginary. To prove (i), we consider $\alpha, \beta \in P_j$

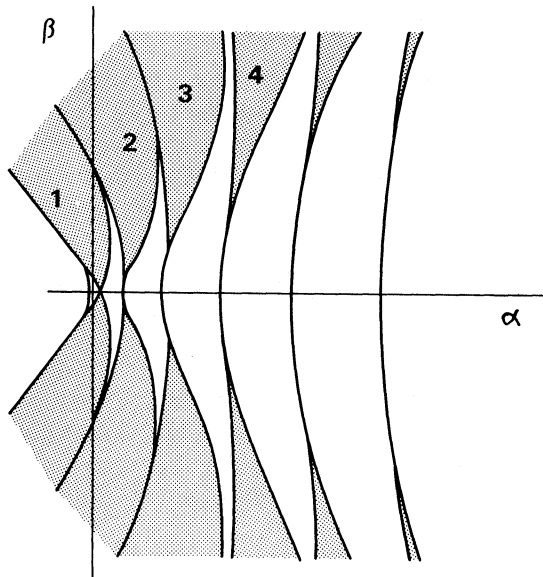


FIG. 3.1. "Stability" diagram for Mathieu's equation. Shaded regions represent parameter ranges where solutions to (3.11) grow exponentially and correspond to $n:1$ phaselocking of (3.7). Numbers represent the rotation numbers.

and recall that the solutions to (3.11) are completely described by Floquet theory [24]. The general solution is:

$$(3.12) \quad V(\tau) = D_1 e^{\nu_1 \tau} Q_1(\tau) + D_2 e^{\nu_2 \tau} Q_2(\tau)$$

where $\nu_1 > 0$ and $\nu_2 < 0$ and $Q_1(\tau), Q_2(\tau)$ are periodic of period T or $2T$ depending on whether j is odd or even. Furthermore, it follows from the oscillation theorem and Sturm theory [24] that $Q_1(\tau)$ and $Q_2(\tau)$ have exactly j zeros in $[0, T)$. If we go back to the θ variable, using (3.9), we see that

$$(3.13) \quad \theta(\tau) = -2 \tan^{-1} \left[\frac{D_1(\nu_1 Q_1 + Q_1') + D_2 e^{(\nu_2 - \nu_1)\tau} (\nu_2 Q_2 + Q_2')}{D_1 Q_1 + D_2 e^{(\nu_2 - \nu_1)\tau} Q_2} \right].$$

Since $\nu_2 - \nu_1 < 0$, it is easy to see that if $D_1 \neq 0$, $\theta(\tau)$ exponentially approaches the stable periodic solution:

$$(3.14) \quad \theta_s(\tau) = -2 \tan^{-1} \left(\frac{\nu_1 Q_1 + Q_1'}{Q_1} \right).$$

There is also an unstable periodic solution, $\theta_u(\tau)$ given by $D_1 = 0, D_2 \neq 0$. Since $Q_j(\tau)$ has exactly j zeros in $[0, T)$, the argument of $\tan^{-1}(\)$ “blows up” j times in the interval, so $\theta(\tau)$ passes $\theta = \pi$ exactly j times. It is easy to check that $\theta'_s(\tau) > 0$ when $Q_1 = 0$ (i.e., $\theta = \pi$); hence $\theta_s(\tau)$ wraps j times around \bar{S}_1 for $\tau \in [0, T)$, i.e. one cycle around L .

To prove (ii), we consider (3.13). As α, β approach the boundary of an instability region, $\nu_1 - \nu_2 \rightarrow 0$. Furthermore, $Q_1(\tau) - Q_2(\tau) \rightarrow 0$ (at a stability boundary there is only one periodic solution to (3.11)). Hence $\theta_s(\tau)$ and $\theta_u(\tau)$ coalesce at the boundary. That they disappear is a consequence of part (iii), i.e. existence of parallel flow for (α, β) in the stability regimes.

(iii) It is clear that for $(\alpha, \beta) \in P_j$ (respectively P_{j+1}), the rotation number is j (respectively $j + 1$). Furthermore, since θ is an increasing function of α , the rotation number is a nondecreasing function of α . Since any point in C_j lies on a line of constant β joining points of P_j to points of P_{j+1} , it follows that, for any point in C_j , the rotation number lies between j and $j + 1$. (As α increases, it takes on all values between j and $j + 1$.)

Finally, if $(\alpha, \beta) \in C_j$, the Floquet exponents of (3.11) are imaginary so the monodromy matrix of (3.11) is equivalent under a change of coordinates to a rotation. The induced change of coordinates on \bar{S}_1 (via (3.9)) takes the time T map of (3.8) onto a rotation. This implies that for these values of (α, β) , (3.8) is equivalent under a change of coordinates to parallel flow. \square

Remark 1. It may be noted that the transformation $x_1 \rightarrow \theta$ and $\theta \rightarrow V$ may be done more transparently by the sequence $x_1 = \epsilon u$ (with only terms of lowest order in ϵ retained), followed by $u = -V_\tau / V$. The first stretches x_1 near $x = 0$ (corresponding to a singular perturbation type of scaling for the “outer” equation), and results in terms quadratic in u plus a time-dependent term (Riccati equation). The second transformation is a standard trick for Riccati equations. The difficulty with this formulation is that the domains for both the u and V variable are unbounded. Since the orbits in question for the x_1 variable traverse the entire domain S^1 of x_1 , this means that the solution must pass, perhaps many times, through the region in which u is not small and $O(u^3)$ terms cannot be ignored. By using the transformation $x_1 = A(\theta, \epsilon)$, a mapping related to the Prüfer transformation [26], one takes a compact domain into another compact domain and “localizes” the “bad” region to a neighborhood of $\theta = \pi$. We

are thus in a position to discuss the convergence as $\varepsilon \rightarrow 0$ of the solution of (3.1) and (3.2) to those of (3.3) and (3.4). This is done in Lemma 4.

For $(\alpha, \beta) \in \text{Int}(P_j)$, there is a stronger convergence result than for $(\alpha, \beta) \in C_j$.

LEMMA 4. (i) Suppose $\tilde{g}(0, y, 0)$ is given by (3.9) with $(\alpha, \beta) \in \text{Int}(P_j)$ for some j . Then for ε sufficiently small there is a periodic solution to (3.1) and (3.2) which converges as $\varepsilon \rightarrow 0$ to the stable periodic solution of (3.3) and (3.4) (or equivalently (3.7)).

(ii) For any (α, β) and $\delta > 0$ sufficiently small, $\exists \varepsilon$ and $0 < k < 1$ such that if $\theta(\tau)$, $y(\tau)$ is any solution to (3.6), (3.2) with $y(0)$ within $k\delta$ of the limit cycle L of (3.4) then $y(\tau)$ stays within δ of L for all τ . Let $\tilde{\theta}: \mathbb{R}^1 \rightarrow \mathbb{R}^1$ be a lift of $\theta(\tau)$. Then $\overline{\lim}((1/\tau)\tilde{\theta}(\tau))$ and $\underline{\lim}((1/\tau)\tilde{\theta}(\tau))$ converge to $\rho(\alpha, \beta)$ as $\delta, \varepsilon \rightarrow 0$.

Proof. We first define a Poincaré map $\mathcal{P}_0: \bar{S}_1 \times U \rightarrow \bar{S}_1 \times U$ for the flow (3.3) and (3.4), where U is a $(q-1)$ -dimensional cross-section transverse in \mathbb{R}^q to the periodic orbit of (3.4). Then $\bar{S}_1 \times U$ is a cross-section for the full system (3.3) and (3.4). As usual, \mathcal{P}_0 takes a point $(\theta, y) \in \bar{S}_1 \times U$ into the next intersection of the trajectory of (3.3) and (3.4) through (θ, y) with $\bar{S}_1 \times U$. (Note that the existence of a stable periodic orbit of (3.4) guarantees that there is such an intersection.) By assumption, $(\alpha, \beta) \in \text{Int}(P_j)$, so (3.3) and (3.4) has a stable periodic point (θ_0, y_0) of \mathcal{P}_0 . By appropriate choice of cross-section we may assume $\theta_0 \neq \pi$.

Next we define a Poincaré map, \mathcal{P}_ε for (3.1) and (3.2) in a similar manner, where U is still taken to be transverse to the periodic orbit of (3.4). We show that \mathcal{P}_ε is well defined and that it is a C^0 perturbation of \mathcal{P}_0 . Since a C^0 perturbation of a map with a hyperbolic fixed point has a nearby fixed point, this will show that \mathcal{P}_ε has such a fixed point, which in turn corresponds to the desired periodic solution to (3.1) and (3.2).

To show that \mathcal{P}_ε is a C^0 perturbation of \mathcal{P}_0 (and at the same time that \mathcal{P}_ε is well defined), we return to the estimates derived in the proof of Lemma 2. For $|\tan(\theta/2)| \leq 1/\sqrt{\varepsilon}$, equations (3.1) and (3.2) converge to (3.3) and (3.4) and hence so do their respective trajectories. Now consider

$$(3.15) \quad \tan \frac{\theta}{2} \cong 1/\sqrt{\varepsilon}.$$

We have seen that (3.15) holds only for an interval of size $4\sqrt{\varepsilon} + O(\varepsilon)$. Furthermore, for θ satisfying (3.15) and $y \in N_1$ (containing L in its interior), $d\theta/d\tau \cong 1$ for ε sufficiently small, by construction (see Lemma 2). Hence, the time (in τ) necessary to pass through the region defined by (3.15) is $\cong O(\sqrt{\varepsilon})$. In this region, (3.2) is bounded for all ε sufficiently small (though not necessarily close to (3.4)). Therefore, y changes by $\cong O(\sqrt{\varepsilon})$ as the trajectory passes once through this region. This shows that for any fixed, finite number of times through the region (3.15), the trajectories of (3.1) and (3.2) with initial conditions near that of the periodic solutions to (3.1) and (3.2) stay arbitrarily close to the latter if ε is sufficiently small. This shows that \mathcal{P}_ε is well defined and a C^0 -perturbation of \mathcal{P}_0 . (It is not a C^1 perturbation due to the fact that large derivatives can occur for (3.1) and (3.2) but not for (3.3) and (3.4) in passing through (3.15).)

We now drop the assumption that $(\alpha, \beta) \in \text{Int}(P_j)$. Let τ_0 be the minimal time it takes any solution to (3.8) with this (α, β) to make one cycle in θ from $\theta = \pi$ to $\theta = \pi$. (This number exists for $(\alpha, \beta) \in C_j$ because the flow is equivalent to parallel flow.) The stability of the limit cycle L of (3.4) then implies that for δ sufficiently small, there is $0 < k < 1$ such that if $\theta(\tau)$, $y(\tau)$ is any solution (in θ, y variables) to (3.1), (3.2), and $y(\tau_1)$ is within δ of L , then for $\tau_2 > \tau_0/2$ one has $y(\tau_1 + \tau)$ is within $k\delta$ of L , provided that $\theta(\tau) \neq \pi$ for $\tau \in [\tau_1, \tau_1 + \tau_2]$. Now previous estimates (in the argument for $(\alpha, \beta) \in$

P_j) imply that y changes by $O(\sqrt{\varepsilon})$ as θ passes through a region around $\theta = \pi$. Thus, for ε sufficiently small, trajectories with initial conditions within $k\delta$ of L cannot get further than δ from L as θ goes once past $\theta = \pi$; as discussed above, the distance to L will then decay to within $k\delta$ before the next time θ passes $\theta = \pi$. Thus, $y(\tau)$ stays within δ of L for all τ .

The statement about the generalized rotation numbers now follows from continuity. \square

Remark 2. Lemma 4 says that solutions to the full equations (3.1), (3.2) are perturbations of solutions to (3.3), (3.4). However, solutions to (3.1), (3.2) do not necessarily stay on the torus defined by $y = y(\tau)$ (i.e. $y \in L$); indeed, there need be no invariant 2-dimensional torus for the full system. In the special case that $h(x, y, \varepsilon)$ is independent of x , there is such a torus; in that case, the parallel flow associated with $(\alpha, \beta) \in C_j$ when $\varepsilon = 0$ can be expected to perturb into phase-locked behavior corresponding to a rational rotation number between j and $j + 1$. In general, however, the solutions to (3.1), (3.2) are C^0 perturbations of solutions to (3.3), (3.4), and a C^0 perturbation of the flow of (3.3), (3.4) can be chaotic. To see how this can occur, we refer to some ideas discovered by Aronson et al. [27] and discussed by Ostlund et al. [28].

For $(\alpha, \beta) \in P_j$ for some j , the Poincaré map \mathcal{P}_0 of (3.3), (3.4) is as in Fig. 3.2. In this picture, there are two critical points, one sink and one saddle, corresponding to the stable and unstable limit cycles of (3.3), (3.4) found above. For (α, β) near a boundary of P_j , these critical points are arbitrarily close; this implies that one of the eigenvalues at the sink is real and close to zero. Since the other $q - 1$ eigenvalues correspond to the Floquet exponents for the limit cycle L , they are by hypothesis bounded away from zero. It follows that a q -dimensional neighborhood of the sink has a “strong stable foliation”, i.e. it can be written as the union of $(q - 1)$ -dimensional “leaves” with the property that two points belong to the same leaf if and only if the distance between their images converges to zero faster than the exponential rate associated with the “slow” eigenvalue of the sink [29].

The saddle point of (3.1), (3.2) has one positive real eigenvalue; its “unstable manifold” W^u consists of two one-dimensional branches, both of which have the sink in its closure; both of these branches are transverse to the strong stable foliation. (See Fig. 3.2.) Now consider a C^0 perturbation of the flow (or equivalently, a C^0 perturbation of \mathcal{P}_0) which introduces into the longer branch of W^u a small “hook”, or local change, such that W^u is quadratically tangent to the strong stable foliation rather than transverse

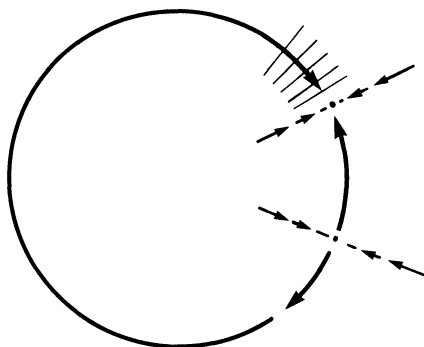


FIG. 3.2. A schematic picture of the Poincaré map \mathcal{P}_0 of (3.3), (3.4) for $(\alpha, \beta) \in P_j$. Since (3.3), (3.4) has a smooth invariant torus, \mathcal{P}_0 has a smooth invariant circle.

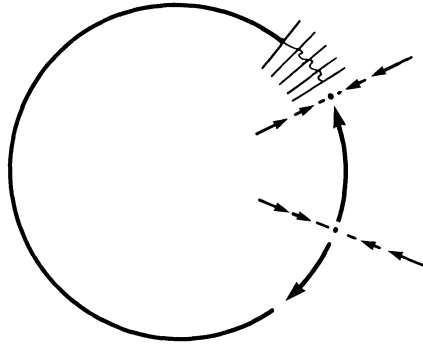


FIG. 3.3. A C^0 perturbation of Fig. 3.2. Note that there are still two critical points, but there need not be a smooth invariant circle.

to it. (See Fig. 3.3.) Note that the existence of one “hook” implies the existence of countably many, since the image of a point of tangency is also such a point.

For these parameter values (i.e. $(\alpha, \beta) \in P_j$), the observed dynamics are still stably periodic and the behavior of the unstable manifold of the saddle is not relevant to the observed dynamics. However, when the parameter values are changed so that now $(\alpha, \beta) \in C_j$, the resulting dynamics, instead of being quasi-periodic, can be chaotic. More precisely, suppose that $(\alpha, \beta) \in \partial P_j$, with $(\alpha + \mu, \beta) \in C_j$. If a C^0 perturbation is made as above for each μ , then a result of Newhouse et al. [30] implies that there is a sequence of $\mu_i \rightarrow 0$ such that the perturbed system has a horseshoe. (For a more complete discussion, see [28].) Of course, to show that these horseshoes actually occur in (3.3), (3.4), one would have to show that by appropriate choices of $g(x, y, \varepsilon)$ and $h(x, y, \varepsilon)$, the resulting C^0 perturbation has the desired properties.

Remark 3. For $(\alpha, \beta) \in P_j$, the limit cycle of (3.8) corresponds to periodic bursting (with j spikes per burst) for equations (2.1), (2.2). Each 2π change in θ corresponds in (x, y) coordinates to one cycle around S^1 ; a spike occurs when θ passes $\theta = \pi$.

In (x, y) coordinates, solutions to (3.8) with $(\alpha, \beta) \in C_j$ correspond to solutions to (2.1), (2.2) having a mixture of j bursts and $(j+1)$ bursts. Since the flow is equivalent to parallel flow on the torus, the sequence of j 's and $(j+1)$'s for (3.8) are determined by the rotation number (and the initial condition); one cannot find a solution with a prescribed sequence of j and $(j+1)$ bursts. However, as discussed in the previous remark, for $(\alpha, \beta) \in C_j$, a perturbation of (3.3), (3.4) may contain horseshoes. Thus, a richer set of sequences of j and $(j+1)$ bursts may be possible for (2.1) and (2.2) (equivalently, (3.1), (3.2)) than for the limiting equations, (3.3), (3.4).

Remark 4. For fixed $\varepsilon > 0$, Lemma 4 establishes only a finite sequence $P_0, C_0, P_1, C_1, \dots$ for which the full equations converge (nonuniformly) to (3.8); the length depends both on the Floquet multipliers of the limit cycle L and the strength of the attraction of the invariant circle S^1 . For $\varepsilon > 0$, the behavior is not specified for (α, β) near the boundary of a region. That is, $(\alpha, \beta) \in P_j$ implies there is a solution to (3.1), (3.2) which converges, as $\varepsilon \rightarrow 0$ to a periodic solution. However, since, for $\varepsilon = 0$, one of the Floquet multipliers converges to 1 as (α, β) approaches a boundary point of P_j , for $\varepsilon > 0$, the corresponding equation need not have a periodic solution. In the special case $h = h(y, \varepsilon)$, the flow reduces to a periodically forced system for x , with phase space $S^1 \times L = T^2$. Then one could define the regions P_j, C_j for $\varepsilon > 0$ using the rotation number ($(\alpha, \beta) \in P_j$ if $\rho = j$), and so $(\alpha, \beta) \in P_j$ implies the equation has a solution with j spikes per burst.

In the special case that $h(x, y, \varepsilon)$ is independent of x , the reduction from (2.1) to (3.1) can be carried out, with the relevant phase space the torus $S^1 \times L$, even if $g(x, y, \varepsilon) = O(1/\varepsilon)$. By appropriate choice of g , the rotation number of the torus, and hence the number of spikes per period, can be arbitrarily high. Thus we see that, if $h(x, y, \varepsilon)$ is independent of x , the analysis will go through for $j \cong \kappa/\varepsilon$, where κ depends on the strength of attraction S^1 . If $j = O(1/\varepsilon)$, the average interspike interval is $O(1)$ in the unscaled time; for $|\beta| \ll \alpha$, this corresponds to regular rapid beating oscillations.

If $h(x, y, \varepsilon)$ is not independent of x , there is the additional problem of convergence of (3.1), (3.2) to (3.3), (3.4). Here, the strength of attraction of L plays a role: the closer to zero the largest Floquet multiplier, the more times $\theta(\tau)$ can pass through the zone around $\theta = \pi$ without moving $y(\tau)$ appreciably from L , and hence the larger j can be and still allow the convergence of Lemma 4 to hold.

Much of the preceding can be summarized by:

THEOREM. *Equations (2.1), (2.2) embed in a 2-parameter family of equations such that, for any j (and $\varepsilon = \varepsilon(j)$ sufficiently small) there are parameter values for which the solutions are bursting solutions with j spikes per burst, or mixtures of j and $(j + 1)$ spikes per burst. The regimes with j spikes per burst are periodic; the others may be periodic for some parameter values, or have “windows” of periodicity with more complex periodic solutions.*

Finally, we show why this mechanism gives rise to parabolic bursting. More accurately, the bursting need not be parabolic under the full generality of (2.1), (2.2); however, an extra qualitative hypothesis suffices to get the conclusion. This hypothesis is that $H(\tau)$ is “qualitatively sinusoidal”, i.e., it is periodic with one relative maximum and one relative minimum per period, with no large changes in slope on a faster time scale.

We recall that, under the inverse of the change of coordinates $x_1 = A(\theta, \varepsilon)$, a small neighborhood of $x_1 = 0$ gets mapped onto all of \bar{S}_1 except a small neighborhood of $\theta = \pi$. A single spike corresponds to a part of a trajectory for which x_1 goes once around S^1 , and hence for which θ passes $\theta = \pi$. The interspike intervals correspond to the time spent with $x_1 \approx 0$ (in the original variables) or θ outside a neighborhood of π (in the changed variables).

PROPOSITION. *If at some τ , $\theta(\tau) < 0$, then $\theta(\tau)$ will not pass $\theta = 0$ until $\alpha + \beta H(\tau) > 0$. (Hence there is no repeated spiking for $\{\tau | \alpha + \beta H(\tau) < 0\}$.) In $\{\tau | \alpha + \beta H(\tau) > 0\}$, interspike intervals decrease with increasing $\alpha + \beta H(\tau)$. Hence, if $H(\tau)$ is qualitatively sinusoidal, the spiking frequency is “parabolic”: it first increases then decreases.*

Proof. The first statement is immediate from (3.7), and the other follows since $\dot{\theta}$ is an increasing function of $\alpha + \beta H(\tau)$. (Recall that on the τ time scale, spikes are instantaneous; for an (α, β) for which there are many spikes per burst, the interspike interval is small relative to the burst period T .) \square

Remark 5. The above argument really relates the variation in interspike intervals to the shape of $\bar{g}(0, y(\tau), 0) = \alpha + \beta H(\tau)$. It also shows that if $\bar{g}(0, y(\tau), 0)$ is not qualitatively sinusoidal, the interspike intervals need not be parabolic. For example, if $H(\tau)$ is as in Fig. (3.4a), the pattern of spiking might be as in Fig. (3.4b).

4. An example. In this section, we present some of the results of the previous section through an illustrative example. In particular, we study the effects of gradually increasing the amplitude of the slow driving oscillator when the burster is excitable. We take as the driving oscillator the piecewise constant function

$$(4.1) \quad H(\tau) = \begin{cases} 1, & 2n \leq \tau < 2n+1, \\ -1, & 2n+1 \leq \tau < 2n+2, \end{cases} \quad n \in \mathbb{Z}.$$

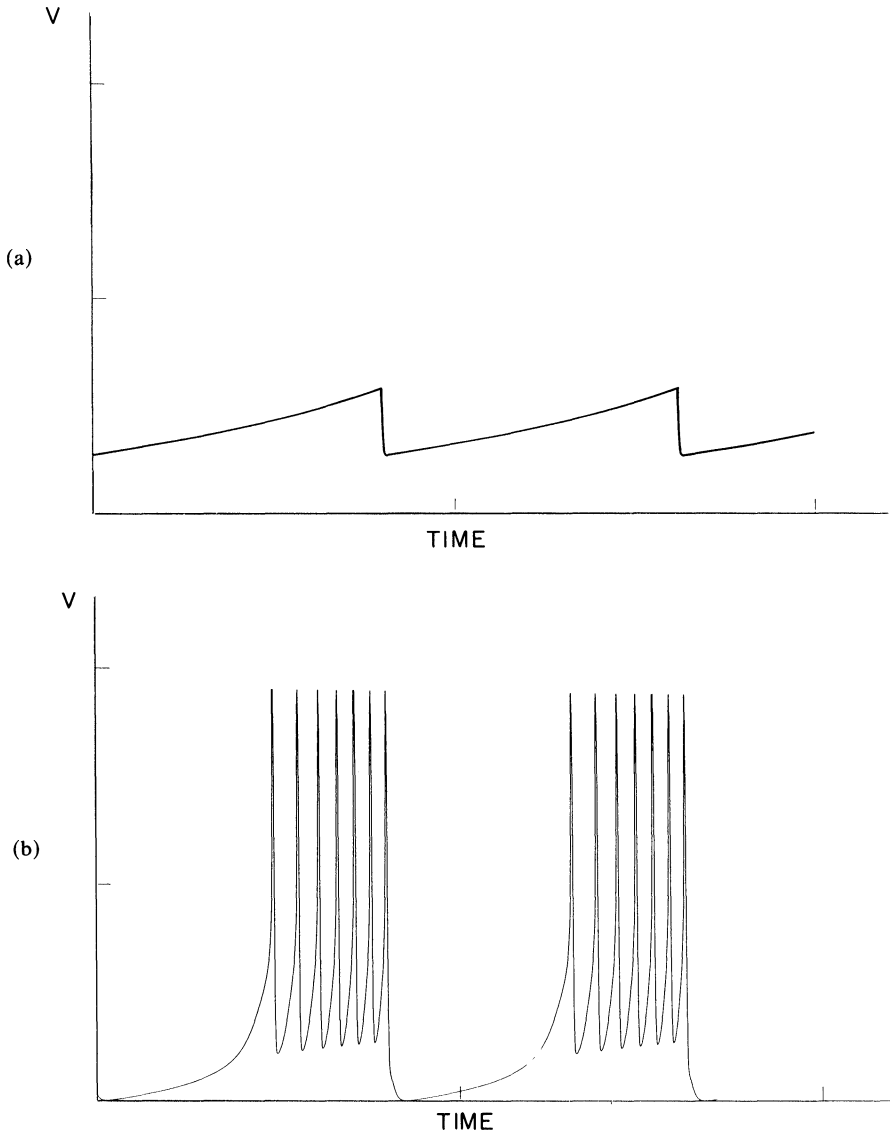


FIG. 3.4. Dependence of bursting pattern on the shape of the slow wave. (a) "Triangular" slow wave. (b) Solutions to equation (4.9) with triangular wave input showing nonparabolic bursting.

The relevant Hill equation is

$$(4.2) \quad \frac{d^2 V}{d\tau^2} = -[\alpha + \beta H(\tau)]V.$$

When $\alpha > 0$, the uncoupled system ($\beta = 0$) is oscillatory or beating and the "cell" fires spontaneously. When $\alpha < 0$, the "cell" is excitable. Only sufficiently large stimuli elicit a spike. We now study the effect of square wave periodic modulation. Numerical experiments with other periodic functions indicate a qualitatively similar behavior. While other forcing functions do not necessarily have the detailed structure of the square wave forcing they share many common features. (For instance, compare Figs.

3.1 and 4.1. Note that in the Mathieu equation the modulation is sinusoidal.) Since (4.2) has an explicit solution, we use it as an example of the forced behavior. From (3.12), we observe that the solution to (4.2) is

$$(4.3) \quad V(\tau) = D_1 e^{\nu_1 \tau} Q_1(\tau) + D_2 e^{\nu_2 \tau} Q_2(\tau)$$

where ν_k are the Floquet exponents and Q_k are periodic functions of τ . We now calculate ν_k as a function of (α, β) in order to understand the phaselocking picture. We recall some results from Floquet theory. Let $(V_1(\tau), V_1'(\tau))$ satisfy (4.2) with $V_1(0) = 1, V_1'(0) = 0$ and let $(V_2(\tau), V_2'(\tau))$ satisfy (4.2) with $V_2(0) = 0, V_2'(0) = 1$. The matrix $M = [(V_1(2), V_1'(2)), (V_2(2), V_2'(2))]$ is the Floquet matrix (the period of the above oscillation is 2). The eigenvalues of M are $\omega_k = e^{\nu_k}$. Since $\det(M) = 1$, ω_k satisfy

$$(4.4) \quad \omega^2 - (V_1(2) + V_2(2))\omega + 1 = 0.$$

From our discussion in § 3, we know that real eigenvalues, ω_1, ω_2 correspond to phaselocked solutions to (3.3) and (3.4) with j spikes per burst for some j . From (4.4), ω_k are real if and only if

$$V_1(2) + V_2(2) \geq 2$$

since the discriminant of (4.4) will be nonnegative. Note that if ω_k are complex, the condition $\omega_1 \omega_2 = 1$ demands that

$$(4.5) \quad \omega_k = \cos \kappa \pm i \sin \kappa.$$

We return to this case shortly.

The parameters (α, β) fall into 3 distinct classes (in each case $\beta > 0$ since $\beta < 0$ is equivalent by a phase shift):

- (i) $\alpha + \beta < 0$ (excitable, weak forcing),
- (ii) $\alpha + \beta > 0, \alpha - \beta > 0$ (oscillatory, weak forcing),
- (iii) $\alpha + \beta > 0, \alpha - \beta < 0$ (strong forcing).

For case (i), the amplitude of the forcing is never sufficient to cross “threshold” so only subthreshold oscillations occur. The remaining two cases describe regions of interesting behavior. By solving (4.2) it is easy to compute $V_1(2) + V_2(2)$ as a function of α and β . Let $r^2 = |\alpha - \beta|$ and $S^2 = |\alpha + \beta|$. Then

$$(4.6a) \quad \frac{1}{2} (V_2(2) + V_2'(2)) = f_1(r, s) = \cos(r) \cos(s) - \frac{1}{2} \left(\frac{r}{s} + \frac{s}{r} \right) \sin(r) \sin(s),$$

$$0 \leq \beta \leq \alpha,$$

$$(4.6b) \quad \frac{1}{2} (V_2(2) + V_2'(2)) = f_2(r, s) = \cosh(r) \cosh(s) + \frac{1}{2} \left(\frac{r}{s} - \frac{s}{r} \right) \sinh(r) \sinh(s),$$

$$\beta > \alpha > -\beta.$$

Note that (4.6) is even in both r and s , so the signs of r and s need not be specified. Equation (4.6a) corresponds to case (ii) and (4.6b) to case (iii). The boundaries between the phase-locked solutions (P_j) and non-phase-locked flow (C_j) are described by the critical curves

$$(4.7) \quad f_1(r, s) = 1, \quad f_2(r, s) = 1$$

since these correspond to the trace being equal to 2. Since (4.6) is even in both r and s and (4.6a) is invariant under a switch between r and s , we may place the solutions to (4.7) on the same graph. The first quadrant in Fig. (4.1) corresponds to (r, s) for

which $f_1(r, s) = 1$ and the second quadrant corresponds to $f_2(r, s) = 1$. We have drawn lines which correspond to $\alpha = 0$ and $\beta = 0$ to orient the reader. We have also indicated where the medium is oscillatory or excitable. The figure shows that when the medium is excitable, once forcing is large enough to obtain any locking, then regions C_j become very thin and almost impossible to find. There is a nonzero minimal value of β below which no locking can occur in the excitable ($\alpha < 0$) system. The minimum β for all $\alpha \leq 0$ occurs when $\alpha = 0$ and hence from (4.6b) satisfies

$$\cosh \sqrt{\beta} \cos \sqrt{\beta} = 1, \quad \beta > 0.$$

There are "tongues" which touch the line $r = s$ and correspond to values of α from which phase-locked solutions bifurcate at $\beta = 0$. When $\beta = 0$, $r = s = \sqrt{\alpha}$ and (4.6a) becomes

$$\cos^2 \sqrt{\alpha} = 1$$

or $\alpha = \pi^2, 4\pi^2, 9\pi^2, \dots$

In what follows, we describe the behavior in regions C_j between the phase-locked domains. These regions represent parallel flow on the torus. For certain special values of (α, β) one can attain entrainment between the two oscillators: for every m stimuli there are n spikes. This entrainment is only structurally stable when $m = 1$ (i.e., 1:1, 2:1, 3:1, \dots entrainment). This result follows from Lemma 3 of § 3. We can use (4.6) to find curves in (α, β) space along which there is entrainment. We then show that the regions C_j can contain regions of stable subharmonic phase-locked solutions in a full model such as (2.1). We recall that when $(V_1(2) + V_2(2)) < 2$, ω_k have the form (4.5). Since $Q_k(\tau)$ are 2π -periodic, in order for (4.3) and (3.13) to be periodic we must have

$$(4.8) \quad 2i\kappa = 2i\pi n/m.$$

For $\kappa_{n,m} = \pi n/m$, the equations

$$f_1(r, s) = \cos \kappa_{n,m}, \quad f_2(r, s) = \cos \kappa_{n,m}$$

determine the curves for $n:m$ entrainment. For then, $\omega = \cos \kappa_{n,m} \pm i \sin \kappa_{n,m}$ as is required. $2\kappa_{n,m}/2\pi$ is the rotation number for the flow on the torus. Once again, we use (4.6a, b) to find the entrainment curves and plot them as was done in Fig. (4.1). In Fig. (4.2) we have plotted $n:5$ entrainment curves for various values of n .

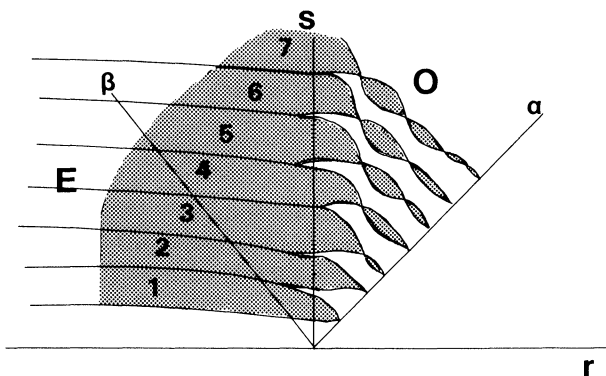


FIG. 4.1. Regions of $n:1$ phase-locking for a square wave slow oscillation. Numbers 1-7 represent the rotation numbers in the shaded regions. The left of the line β labeled "E" is the region where the medium is excitable (" $\alpha < 0$ ") and to the right, labeled "O" it is oscillatory (" $\alpha > 0$ "). r and s are as in text.

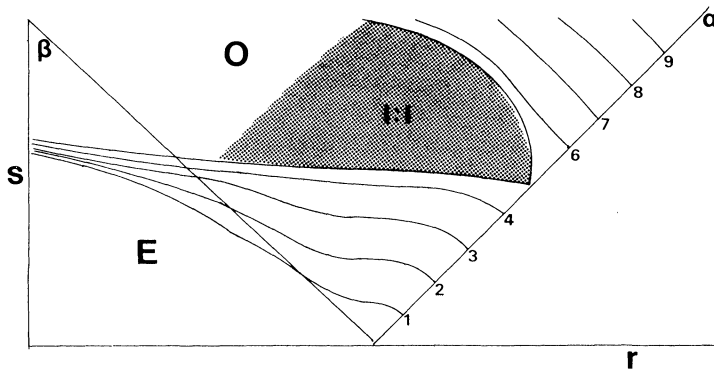


FIG. 4.2. Curves of rational rotation number of the form $n/5$ for square wave form slow oscillations. Shaded region is 1:1 phase-locked. (See Fig. (4.1) and text for additional details.)

We now describe the behavior of a real model in the regions for which (4.1) has parallel flow. This model is a nerve conduction equation for the mitral cell axons derived by Rall and Shepherd [18] and used in a related study by Rall and Goldstein [13]. The system described by Rall and Shepherd is third order but one variable is faster than the others so we can reduce it to a second order equation:

$$(4.9) \quad \begin{aligned} \frac{dV}{dt} &= -V + 1200V^4(1 - V) - J(V + .1) + I(t), \\ \frac{dJ}{dt} &= 8.5(1200V^4 - 2J). \end{aligned}$$

In the numerical examples below $I(t) = I_0 + a + bH(\tau/T)$. $I_0 = .047$ is the value for which (4.9) satisfies Hypothesis A in § 3. We put $a = -.045$ so that the system is excitable and gradually raise b above 0. There is a range of values of b for which there are periodic solutions to (4.9) with rotation numbers that are less than 1. These also appear to be structurally stable. We have obtained 1:3, 2:3 and 1:2 stable subharmonic solutions to (4.9) for small b . Note that (4.9) is an example of a forced excitable system; there is no feedback from the excitable system to the slow oscillation.

5. Discussion. We have described a general model for the bursting observed in several biological and chemical systems. Our hypotheses are simple: the existence of an excitable spiking mechanism coupled to an underlying slow oscillation. Several qualitative aspects of bursting behavior are easily recovered from our model. The proposition of § 3 shows how the “threshold” of threshold models (e.g. [31]) is made explicit and how it changes with parameters. Consider for example, $(\alpha, \beta) \in P_j$. For large β and small α , within P_j the j spikes are bunched into a small interval of phases. This gives a “burstlike” qualitative picture of the spiking. For α large and β small, within P_j the amplitude of the periodic modulation is small and the spikes occupy almost all of the slow period. As $\beta \rightarrow 0$ the spikes become uniformly distributed. So within the region P_j one can change parameters (α, β) and go from a “bursting” solution to a “beating” solution. This shows that the distinction between beating and bursting is one of degree, not kind; there need be no bifurcation that separates a beating solution from a bursting one.

Our model for the spiking mechanism and excitability, “saddle-point excitability”, is somewhat novel. We assume the existence of a “circle in resonance”, i.e. an invariant

circle containing a stable node and a saddle point. (For $x \in \mathbb{R}^2$, this implies the existence of a third critical point, a source.) This contrasts with the better known model for excitable media in which there is but one steady state. The latter is the mechanism underlying the Fitzhugh–Nagumo equations, the standard Hodgkin–Huxley equations, and the Field–Noyes–Koros equations to the Belousov–Zhabotinskii reaction. “Saddle point excitability” has been suggested by Rinzel and Ermentrout (unpublished) as the mechanism for excitability and oscillation in class I nerve axons [22].

There are many properties which distinguish the present mechanism of excitability from the better known model. In both cases, small perturbations of the excitable system yield an oscillatory system; however, for saddle point excitability, the oscillations come via a saddle-node bifurcation, while for the better known model it is via a Hopf bifurcation. From this, one can see that resulting oscillations can have arbitrarily low frequency for our model, but not for the other. Furthermore, beyond the bifurcation, the oscillations in our case all have large amplitude. (They follow the “circle in resonance”.) By contrast, the oscillations via the Hopf bifurcation are initially small. When the two types of excitable systems are slowly forced, one sees different behavior: In our case, the spikes in a burst are all large amplitude, while for the other, the spikes at the beginning and end of each burst are small amplitude. Another property of our mechanism of excitability is “infinite latency”: because of the saddle point, there are initial conditions for which there is an arbitrarily long time before a spike is generated. This is not true of the other mechanism.

Coupled to the spiking mechanism is the slow oscillation. In [7] we review evidence for such an underlying modulation in several systems which include the bursting cell of aplysia and the oscillations in mammalian smooth muscle. As was shown in § 3, the shape of this oscillation determines the interspike interval during a burst. In particular, if $H(\tau)$ is sinusoidal, parabolic bursting is observed. In addition to parabolic bursting we can account for many of the details which are experimentally observed in bursting preparations if we specialize the equations $\dot{x} = f(x)$ of Hypothesis A to a Hodgkin–Huxley like system [7]. To understand some experimental observations in terms of our model, it is necessary to hypothesize that the slow oscillation be modifiable by the variables of the excitable system (e.g. voltage), that is, that $h(x, y, \varepsilon)$ not be wholly independent of x . We note that most of the mathematical features of (2.1), (2.2) occur already in the simpler system in which h is independent of x . (One exception is the possibility of chaos.) The dependence of h on x makes the results harder to establish. We prove them in the above generality because of the evidence that, for the applications we envision [7], the slow oscillations *can* be modified by external perturbation of the voltage.

We note that although the model was invented to describe the interactions of a cytoplasmic oscillation with the membrane properties in a single cell, the formalism works equally well in describing two types of cells, one of which oscillates slowly, and the other of which is excitable. Such a pair is thought to form the essential part of the pacemaker in the pyloric system of the lobster stomatogastric ganglion [32], [33]. The “*AB* cell” oscillates endogenously, often without spikes, with a smooth wave form and a period of the order of a second. A “*PD* cell”, which is excitable, is electrically coupled to the *AB* cell and undergoes parabolic bursting in the intact network (with full sized spikes at the ends of each burst). Marder and Eisen show that these cells respond differentially to stimulation and neurotransmitters, providing a system whose output to other neurons can be flexibly adjusted without changing the “hard wiring”. They suggest that similar networks may be widespread.

There are many other mechanisms which can lead to bursting behavior, [5], [8], [9], [10], some of which have a “parabolic” bursting structure. Carpenter [8] has produced parabolic bursting but her equations describe waves travelling down axons, not the space-clamped situation. Plant et al. [9], [34] derive a model of the parabolically bursting aplysia abdominal cells. The model is based on Hodgkin–Huxley type equations with several additional conductances. Many of the detailed features of the response of the cell to voltage and other perturbations are derived from the models, but not the parabolic interspike intervals.

Several other models of bursting, not necessarily parabolic, exist and the mathematical mechanisms for these are more transparent than those of Plant et al. Recently, Rinzel and Troy [5] and Chay and Rinzel [10] have described models for bursting in the Zhabotinskii reaction and in insulin secreting cells respectively. As in our model and the models of Plant et al., there is a slowly varying quantity. In contrast to our model, in [5] and [10] this quantity does not change in the absence of changes in the variables that are part of the excitable mechanism. In particular, there is no slow limit cycle for any fixed value of the excitable variables. The excitable mechanism of [5] relies on the existence of a subcritical Hopf bifurcation and a large amplitude limit cycle. The slow quantity, which is coupled to the excitable system, acts as a bifurcation parameter; in the coupled system, the parameter oscillates between the unstable and the stable regimes (see Fig. 5.1) in a hysteresis loop. This leads to burstlike behavior. The interspike intervals for these models depend crucially on the amplitude-frequency relationship of the bifurcating limit cycle. In general they are not parabolic.

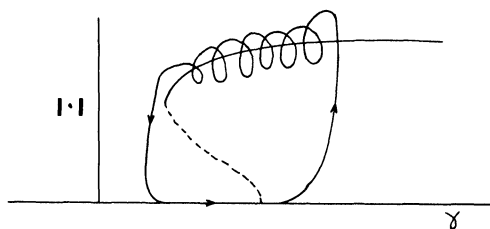


FIG. 5.1. *Bursting mechanism proposed for the FKN equations. There is a subcritical Hopf bifurcation and the parameter γ (flow rate) is allowed to slowly vary. This results in γ moving left and right through the bifurcation diagram. When on the upper branch, the system oscillates at high frequencies and on the lower branch it is quiescent. $|\cdot|$ denotes amplitude.*

Finally, we mention a similarity between the phenomena discussed in the present paper and some experimental results obtained by Turner et al. [3] on the temporal behavior of the Belousov–Zhabotinskii (BZ) reaction when carried out in a continuously-stirred tank reactor. The similarity is not in the mechanism: there is no known driving oscillation. Nor is it in the form of the “bursts”. Rather, it is in the existence of a sequence of regimes analogous to the regions found in Hill’s equation. With fixed initial chemical concentrations, one may obtain different temporal behavior by varying the flow rate r of the tank. As r is increased, one passes through a sequence of regimes $P_1, C_1, P_2, C_2, \dots$. (Only a finite sequence has been found experimentally.) For $r \in P_j$, the temporal output is a complex periodic solution; the output is periodic with one large amplitude and j small amplitude oscillations. For $r \in C_j$, the output is a mixture of j and $(j+1)$ type bursts, as in the mechanism of this paper. Furthermore, for other parameter regimes, Maseko and Swinney [35] find that a “rotation number”, defined as the number of small oscillations divided by the total number of oscillations per

burst, varies monotonically with the flow rate. This is again analogous to the behavior of the class of equations in this paper.

For the Zhabotinskii reaction, spectral analysis shows that, when $r \in C_j$, the behavior is chaotic [3]. This contrasts with (3.8) since flow on a torus cannot be chaotic. It remains to find out if (nonuniform) perturbations of (3.8) in a 3-dimensional space, as in (2.1), (2.2) could display chaos. (As stated above, unless $h(x, y, \varepsilon)$ is dependent on x , the quasi-periodic flow can be expected to perturb for rational rotation numbers to phase-locked solutions.) Rinzel and Schwartz [36] have numerically examined mixing of j - and $(j+1)$ -mode solutions for a bursting model. They use a one-variable discrete time map to describe the behavior of these mixing solutions. Chaos was not identified numerically or analytically in this work.

Acknowledgments. We wish to thank P. Holmes and D. Rand for bursts of conversation, and J. Rinzel for a careful reading.

REFERENCES

- [1] M. J. BERRIDGE AND P. E. RAPP, *A comparative survey of the function, mechanism and control of cellular oscillators*, J. Exp. Biol., 81 (1979), pp. 217-279.
- [2] P. E. RAPP AND M. J. BERRIDGE, *Oscillations in calcium-cycle AMP control loops form the bases of pacemaker activity and other higher frequency biological rhythms*, J. Theoret. Biol., 66 (1977), pp. 497-525.
- [3] J. S. TURNER, J. C. ROUX, W. C. MCCORMICK AND H. L. SWINNEY, *Alternating periodic and chaotic regimes in a chemical reaction*, Phys. Letters, 85A (1981), pp. 9-12.
- [4] J. L. HUDSON, M. HART AND D. MARINKO, *An experimental study of multiple peak periodic and non-periodic oscillations in the Belousov-Zhabotinskii reaction*, J. Chem. Phys., 71 (1979), pp. 1601-1606.
- [5] J. RINZEL AND W. TROY, *Bursting phenomena in a simplified Oregonator flow system model*, J. Chem. Phys. 76 (1982), pp. 1775-1789.
- [6] A. ARVANITAKI AND N. CHALAZONITIS, *Electrical properties and temporal organization in oscillatory neurons*, Symposium on Neurobiology of Invertebrates, J. Salanki, ed., Plenum, New York, 1967, pp. 169-199.
- [7] N. KOPELL AND G. B. ERMENTROUT, *Subcellular oscillators and bursting*, preprint.
- [8] G. A. CARPENTER, *Bursting phenomena in excitable membranes*, this Journal, 36 (1979), pp. 334-372.
- [9] R. E. PLANT AND M. KIM, *Mathematical description of a bursting pacemaker neuron by a modification of the Hodgkin-Huxley equations*, Biophys. J., 16 (1976), pp. 227-244.
- [10] T. R. CHAY AND J. M. RINZEL, *Bursting, beating and chaos in an excitable membrane model*, preprint.
- [11] N. FENICHEL, *Geometric singular perturbation theory for ordinary differential equations*, J.D.E., 31 (1979), pp. 53-98.
- [12] J. A. CONNOR, D. WALTER AND R. MCKOWN, *Neural repetitive firing: modifications of the Hodgkin-Huxley axon suggested by experimental results from crustacean axons*, Biophys. J., 18 (1977), pp. 81-102.
- [13] S. S. GOLDSTEIN AND W. RALL, *Changes of action potential shape and velocity and changing core geometries*, Biophys. J., 14 (1974), pp. 731-757.
- [14] R. FITZHUGH, *Mathematical models of excitation and propagation in nerve*, in Biological Engineering, H. P. Schwan, ed., McGraw-Hill, New York, 1969, pp. 1-85.
- [15] J. M. RINZEL, *Models in neurobiology*, in Lectures in Applied Mathematics, Vol. 19, American Mathematical Society, Providence, RI, 1981, pp. 281-297.
- [16] N. FENICHEL, *Persistence and smoothness of invariant manifolds for flows*, Indiana Univ. Math. J., 21 (1971), pp. 193-226.
- [17] G. B. ERMENTROUT AND J. M. RINZEL, *Waves in a simple, excitable or oscillatory, reaction-diffusion model*, J. Math. Biol., 11 (1981), pp. 269-294.
- [18] W. RALL AND G. M. SHEPHERD, *Theoretical reconstruction of field potentials and dendrodendritic synaptic interactions in olfactory bulb*, J. Neurophys., 31 (1968), p. 884.
- [19] S. P. HASTINGS, *Persistent spatial patterns for semi-discrete models of excitable media*, J. Math. Biol., 11 (1981), pp. 105-117.

- [20] H. C. TUCKWELL AND R. M. MIURA, *A mathematical model for spreading cortical depression*, *Biophys. J.*, 23 (1978), pp. 257–283.
- [21] H. R. WILSON AND J. D. COWAN, *A mathematical theory of the functional dynamics of cortical and thalamic nervous tissue*, *Kybernetik*, 13 (1973), pp. 55–80.
- [22] A. L. HODGKIN, *The local electric changes associated with repetitive action in a non-medullated axon*, *J. Physiol.*, 107 (1948), pp. 164–181.
- [23] R. A. CHAPLAIN, *Metabolic regulation of the rhythmic activity in pacemaker neurons II*, *Brain Research*, 106 (1976), pp. 307–319.
- [24] E. A. CODDINGTON AND N. LEVINSON, *Theory of Ordinary Differential Equations*, McGraw-Hill, New York, 1955.
- [25] W. MAGNUS AND S. WINKLER, *Hill's Equation*, Wiley-Interscience, New York, 1966.
- [26] G. BIRKHOFF AND G. C. ROTA, *Ordinary Differential Equations*, Blaisdell, Waltham, MA, 1969.
- [27] D. G. ARONSON, M. A. CHORY, G. R. HALL AND R. P. MCGEHEE, *Bifurcations from an invariant circle for 2-parameter families of maps of the plane: A computer assisted study*, *Comm. Math. Physics*, 83 (1982), pp. 303–354.
- [28] S. OSTLUND, D. RAND, J. SETHNA AND E. SIGGIA, *Universal properties of transition from quasi-periodic to chaos in dissipative systems*, *Physica*, 8D (1983), pp. 303–342.
- [29] M. W. HIRSCH, C. C. PUGH AND M. SHUB, *Invariant Manifolds*, Lecture Notes in Mathematics, 583, Springer-Verlag, Berlin, 1970.
- [30] S. NEWHOUSE, J. PALIS AND F. TAKENS, *Bifurcations and stability of families of diffeomorphisms*, *I.H.E.S. Publications Math.*, 57 (1983), pp. 5–71.
- [31] D. JUNGE AND C. L. STEPHENS, *Cyclic variation of potassium conductance in a burst generating neuron in aplysia*, *J. Physiol.*, 235 (1973), pp. 155–181.
- [32] E. MARDER AND J. S. EISEN, *Electrically coupled pacemaker neurons respond differently to some physiological inputs and neurotransmitters*, *J. Neurophys.*, 51 (1984), pp. 1362–1374.
- [33] J. S. EISEN AND E. MARDER, *A mechanism for production of phase shifts in a pattern generator*, *J. Neurophys.*, 51 (1984), pp. 1375–1393.
- [34] R. E. PLANT, *The effects of calcium on bursting neurons*, *Biophys. J.*, 21 (1978), pp. 217–237.
- [35] J. MASELKO AND H. L. SWINNEY, *A complex transition sequence in the Belousov-Zhabotinskii reaction*, to appear in *Physica Scripta*, Proc. Nobel Symposium on the Physics of Chaos and Related Problems, June 1984.
- [36] J. RINZEL AND I. B. SCHWARTZ, *One variable map prediction of Belousov-Zhabotinskii mixed mode oscillations*, *J. Chem. Phys.*, 80 (1984), pp. 5610–5615.